Laser-assisted charge transfer in $He^{2+}+H$ collisions

Fatima Anis,* V. Roudnev, R. Cabrera-Trujillo, and B. D. Esry
J.R. Macdonald Laboratory, Department of Physics, Kansas State University, Manhattan, Kansas 66506, USA
(Received 22 December 2005; published 26 April 2006)

The time-dependent Schrödinger equation is solved numerically to investigate laser-assisted charge transfer in $He^{2+}+H+nh\nu$ collisions at 1 keV in the semiclassical impact parameter approach. Laser polarizations parallel and perpendicular to the projectile trajectory are studied. For both polarizations even a moderately intense laser ($I_0=3.5\times10^{12}$ W/cm^2) significantly increases the reaction probability. In addition, we find that the relative collision-laser phase has little influence on the charge transfer. We focus on parameters more favorable to experiment.

DOI: 10.1103/PhysRevA.73.043414 PACS number(s): 34.50.Rk, 34.50.Fa, 32.80.Wr, 34.70.+e

I. INTRODUCTION

The idea of combining atomic collisions with an external laser field has been investigated since the early 1970s, when simultaneous collisional and radiative excitations were suggested to study interatomic interactions [1]. Although further theoretical development [2–5] continued during the 1980s, it was probably the lack of experiments that moderated interest in the topic. Recent progress in experimental techniques have made it possible to probe collision and laser-induced processes in new regimes and also to attain much higher laser intensities. Consequently, these advances have renewed theoretical interest in this long-standing problem of laser-assisted atomic collisions [6–11].

When an asymmetric ion-atom collision occurs in the presence of an intense laser field, the laser-induced charge exchange cross section can become several orders of magnitude larger than the corresponding collision-induced charge exchange cross section [2]. Since the early work of Gudzenko and Yakovenko [1], most attention has been focused on resonant effects where the laser frequency was tuned to some transition in the collision system [2,3,9]. Early calculations were performed for relatively low intensities by today's standards [4], and were based only on two-state treatments in which the laser assisted capture is a consequence of coupling induced by the laser field. Nevertheless, they showed substantial enhancement. More recent work [6,7] has focused on laser intensities above 10^{13} W/cm^2 by using the basis generator method—a nonperturbative method that has been successful in the description of field-free ion-atom collisions—with a CW laser.

One of our main goals for these calculations is to determine whether the laser can significantly modify the collision outcome under conditions favorable to experiments. We expect that the laser intensities required to measurably influence the collision are sufficiently high that pulsed lasers must be used. If a substantial effect can be obtained with a lower intensity, though, longer pulses can be used, increasing the fraction of the time the laser is on and improving the duty cycle. To this end, we will consider here a modest intensity of 3.5×10^{12} W/cm^2. Since we use the laser frequency $\omega=0.057$ a.u., which corresponds to 800 nm Ti:sapphire lasers commonly used, the laser is not resonant with either of the separated fragments, namely He^+ and H. This, combined with the lower laser intensity, has two important consequences: both ionization and excitation by the laser are negligible. We further choose the relatively low projectile velocity of $v=0.1$ a.u. (1 keV) so that ionization during the collision is also negligible. Essentially then, charge exchange is the only inelastic channel possible.

We apply two methods: a lattice solution and the electron-nuclear dynamics (END) approach [12,13]. Our main results are based on the lattice solutions, but we also use this opportunity for the lesser goal of validating the END method for such systems. The END method also serves to double-check the lattice results. We consider the influence of laser polarization on the capture probability, as well as its dependence on the relative collision-laser phase (RCLP). Our calculations demonstrate a significant enhancement of the charge-transfer cross section—even for the modest intensity used.

II. THEORY

A. Lattice approach

A complete quantum mechanical calculation of laser-assisted charge transfer is a computationally difficult problem. For sufficiently high projectile momenta, though, a simplified semiclassical model can be applied. For instance, a trajectory model is a common approach that utilizes a quantum mechanical treatment of the electronic degrees of freedom and a classical treatment of the nuclear degrees of freedom. For projectile energies as low as a few keV, the heavy particle trajectories can be approximated by a straight line characterized by its impact parameter b (see Fig. 1).

In the present case, the interaction with the laser field can be represented within the dipole approximation. The electronic wave function thus satisfies the following time-dependent Schrödinger equation (in atomic units):

$$i\frac{\partial}{\partial t}\Psi(\mathbf{r},t)=[T+V(t)]\Psi(\mathbf{r},t) \quad (1)$$

with

*Electronic address: fatima@phys.ksu.edu

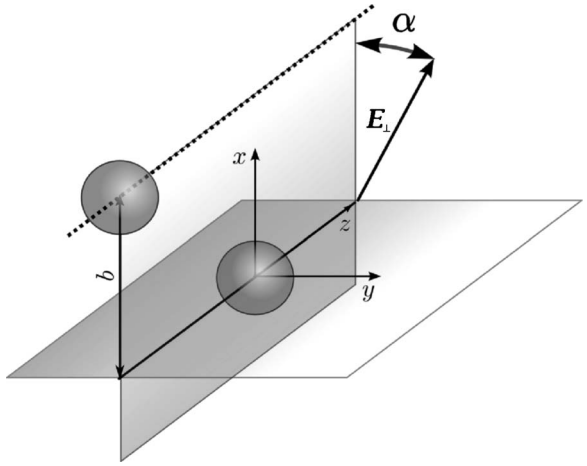

FIG. 1. He^{2+}+H laser-assisted charge transfer collision geometry. The dotted line is the projectile trajectory, b is the impact parameter, $\mathbf{E}$ is the laser field, α is the angle between the laser polarization and the collision plane.

$$T = -\tfrac{1}{2}\nabla^2, \tag{2}$$

$$V(t) = -\frac{Z_T}{|\mathbf{r}|} - \frac{Z_P}{|\mathbf{r} - \mathbf{R}_P(t)|} - \mathbf{E}(t)\cdot\mathbf{d}. \tag{3}$$

In these expressions, Z_T and Z_P are the target and projectile charges, respectively, $\mathbf{R}_P(t)$ is the projectile trajectory, and $\mathbf{d}=-\mathbf{r}$ is the electron dipole operator. In our lattice calculations we place the projectile's straight line trajectory along the z axis, such that $\mathbf{R}_P(t)$ reads

$$\mathbf{R}_P(t) = b\hat{\mathbf{x}} + vt\hat{\mathbf{z}}, \tag{4}$$

where $b>0$ is the impact parameter, v is the velocity of the projectile, and $\hat{\mathbf{x}}$ and $\hat{\mathbf{z}}$ are the unit vectors along the x and z axes, respectively.

The laser field is taken to be a pulse with a Gaussian envelope reaching its peak value at $t=0$, i.e., the point of closest approach between the projectile and the target. Explicitly, we use the following expression for the laser field:

$$\mathbf{E}(t) = \mathbf{E}_0 e^{-(t/\tau)^2}\cos(\omega t + \varphi), \tag{5}$$

where $\mathbf{E}_0$ is the electric field amplitude, $\tau\sqrt{4\ln 2}$ defines the intensity full width at half-maximum (FWHM) duration of the pulse, ω is the carrier frequency, and φ is the phase of the laser field at the time of the closest approach for the collision. We call φ the relative collision-laser phase (RCLP). The RCLP combines both the carrier-envelope phase of the laser as well as the synchronization of the laser pulse with the collision.

Our lattice solution of Eq. (1) utilizes a uniform grid and the three-point finite-difference method [16]. The time evolution is accomplished by operator splitting

$$\Psi(\mathbf{r},t+\delta) = e^{-iV\delta/2}e^{-iT\delta}e^{-iV\delta/2}\Psi(\mathbf{r},t) + O(\delta^3). \tag{6}$$

The unitary Cayley-Hamilton approximant $e^{iA\delta}=(1-\frac{i}{2}A\delta)^{-1}(1+\frac{i}{2}A\delta)+O(\delta^3)$ is used to calculate the operator exponentials. This approach is one generalization of the standard Crank-Nicholson method [14] to several dimensions.

Although this numerical approach appears straightforward, the calculations are computationally intensive and some care must be taken in order to obtain stable and accurate results. One problem arises from the charge traveling through the grid. A moving Coulomb singularity can cause numerical problems if it falls on any of the grid points during the propagation. Even if the singularity misses the grid points, its passage can produce an effective periodic driving as it passes near each grid point. We initially included a softening parameter in the Coulomb potentials to deal with this problem, but found that the charge exchange probability was consistently overestimated. Details of our investigation of this phenomenon can be found in the Appendix. Given these difficulties, we settled on the solution used in Ref. [9], namely placing the trajectories at the center of a square defined by adjacent points in the xy plane. To further minimize numerical fluctuations during the propagation, we worked in the reference frame of the He^{2+} particle by fixing its position with respect to the grid. The changing proton position was less problematic, since its charge is lower. Thus, in our calculations, the H atom is treated as the projectile and the He^{2+} particle as the target. The grid has been chosen such that the He^{2+} lies at the center of a cube of grid points at the origin. This choice of reference frame only introduces an unimportant overall phase factor in the wave function, even in the presence of the laser field.

The uniform grid employed in most of the calculations covered the region $[-4,15]_x\times[-4,4]_y\times[-25,25]_z$ a.u. This region was chosen to balance the accuracy of the physical parameters of the system with the overall computational time. Keeping the latter to a reasonable value simply translates to keeping the grid as small as possible. Since the collision takes place in the xz plane, for instance, the grid range in the y direction can be modest. The former consideration must take into account that the boundaries in z should be far enough to clearly separate the fragments in the final state. Also, none of the grid boundaries should perturb the wave function since we require that the wave function vanish at the boundaries. For this reason, the positive x boundary was extended to 20 a.u. for $b>10$ a.u. [see Eq. (4)]. No boundaries were placed closer than 4 a.u. from either nucleus in order to reproduce the $H(1s)$ and $He^+(2l)$ states with reasonable accuracy. The key point for the grid is that the $He^+(2l)$ states are very close to the same size spatially as the $H(1s)$ state.

Our grid step of 0.2 a.u. gave $E_H=-0.490$ a.u. for the hydrogen ground state energy and $E_{He^+}=-1.90$ a.u. for the ground state of the He^+ ion. This grid also supports a $He^+(2s)$ state with energy -0.489 a.u. and $He^+(2p)$ states with energies -0.470 a.u., and -0.495 a.u. for states aligned along the y, and z axes, respectively. The $He^+(2p)$ state energy aligned along the x axes is half way between the energies of the $2p_y$ and $2p_z$ states. These states are all comparable in accuracy, and very nearly maintain their expected degeneracy. The different ranges of the grid in each direction is the reason that the various $2l$ states are not exactly degenerate. Even though these values are not impressively accurate, they maintain the

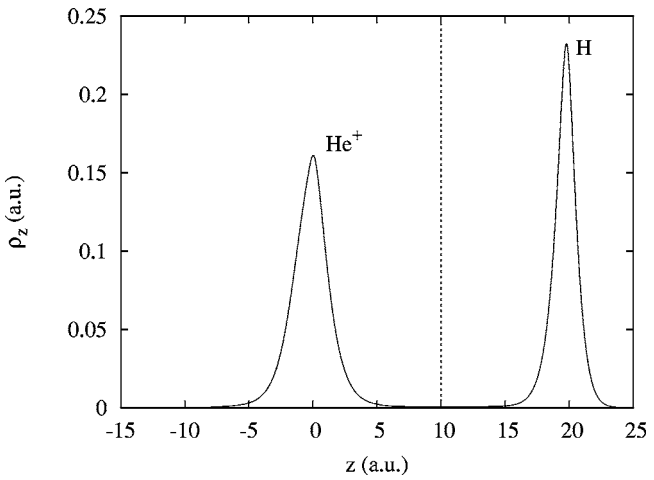

FIG. 2. A typical He^{2+}+H final state density function for $b=0.4$ a.u., RCLP=0, parallel polarization, and a collision energy of 1 keV. The dashed line is the boundary of Ω_T (see text).

essential properties of the real system, and we will argue below that the accuracy is sufficient to estimate the effect of the laser field on the capture probability.

Our calculations covered the time range from $t_i=-200$ to $t_f=200$ a.u. This propagation time is long enough to achieve a clear separation at the final time between the target and the projectile at the projectile velocity of 0.1 a.u. (1 keV). This velocity is used in all our calculations, except for some field-free tests that we shall describe in the next section. We have employed a time step of 0.06 a.u., which gives a reasonable compromise between accuracy and computation time. This time step was chosen on the basis of several tests of energy conservation. In these tests, the laser field was turned off as was either the target or projectile potential. The time step of 0.06 a.u. satisfied energy conservation with relative error of no more than 0.7%. A typical calculation for one configuration takes about 3 hours on a 500 MHz EV7 Alpha workstation.

We calculate the charge exchange probability by integrating the electron density function over a box Ω_T surrounding the target at the final time t_f,

$$P = \int_{\Omega_T} |\Psi(\mathbf{r},t_f)|^2 d^3\mathbf{r} \equiv \int_{z_{\min}}^{z_T} \rho_z(z,t_f) dz, \tag{7}$$

where the density function $\rho_z(z,t)$ is given by

$$\rho_z(z,t) = \int_{x_{\min}}^{x_{\max}} \int_{y_{\min}}^{y_{\max}} |\Psi(x,y,z,t)|^2 \, dx \, dy.$$

When implementing Eq. (7), it is important that the target and the projectile contributions to the wave function must be clearly separated in space so that Ω_T boundary can be placed in the region where both contributions are negligibly small. Since $z=20$ a.u. at t_f for the H atom, we define Ω_T to cover z from $z_{\min}$ to $z_T=10$ a.u. (the midpoint between the two nuclei at t_f) and all x and y. A typical final state probability density is presented in Fig. 2 with the vertical dashed line marking the boundary of Ω_T. Recalling that the initial state was He^{2+}+H, the figure shows that charge exchange has taken place since there is density near the He^{2+} at $z=0$ a.u. Figure 2 also illustrates why the present calculations required no absorbing boundaries—no substantial flux reached the grid boundaries. At the relatively low collision energy and laser intensity under consideration, ionization was negligible.

Some attention must be paid to numerical error in these calculations, especially with the simple method, Eq. (7), we are using to analyze the charge exchange probability. In particular, the moving H atom is only approximately a stationary state numerically. The nonstationary part appears as a more-or-less uniform background density in ρ_z as though the H atom were weakly ionized, which is consistent with an effective driving potential with angular frequency $2\pi v/\Delta x=\pi$ a.u. If this probability were mistakenly included in the capture probability, it could, due to its contribution at large impact parameters, generate significant errors in the cross section. We estimated the magnitude of this error by propagating the H atom through the grid without the He^{2+} and laser. We thus found a probability error of 7×10^{-4}. To compensate this effect, we subtract 7×10^{-4} from all calculated capture probabilities, effectively treating any probability smaller than 7×10^{-4} as zero.

B. The END method

As a second check of the consistency of our results we have supplemented the grid calculations with results obtained within the END method [12,13].

The END method is a many-electron approach to simultaneously treat the electronic and nuclear dynamics. It is based on the time-dependent variational principle to solve the time-dependent Schrödinger equation by deriving a Hamiltonian dynamical system of equations for the time-dependent nuclear and electronic wave functions. The resulting system of coupled, first-order, ordinary differential equations provides an approximation to the Schrödinger equation. The END method uses a parametrization of the wave function in a coherent state manifold and, in its simplest implementation, uses a single determinantal, spin-unrestricted, electronic wave function centered on the dynamically changing nuclear positions. It thus includes the trajectories of the nuclei and their coupling to the dynamic electrons self-consistently. The electric field is treated in the dipole approximation [13] (length gauge). In the present one electron problem, the many-electron nature of the method is, of course, irrelevant.

The electronic wave function is expanded in terms of a Gaussian primitive basis set. For this problem, we have used a $[6s2p/3s2p]$ basis set optimized by Dunning [15] for atomic hydrogen and a $[9s3p2d/7s3p2d]$ basis set for He^+. For the case of He^+, the inclusion of d-orbitals is necessary to have a sufficiently good description of the low excited states ($2l$ and $3l$) largely responsible for the charge exchange process. With this basis set, we obtained ground state energies of $E_H(1s)=-0.4993$ a.u. and $E_{He^+}(1s)=-1.9996$ a.u. This basis also gave He^+ excited state energies of $E_{He^+}(2s)=-0.4987$ a.u. and $E_{He^+}(2p)=-0.4827$ a.u., with all three p orientations exactly degenerate.

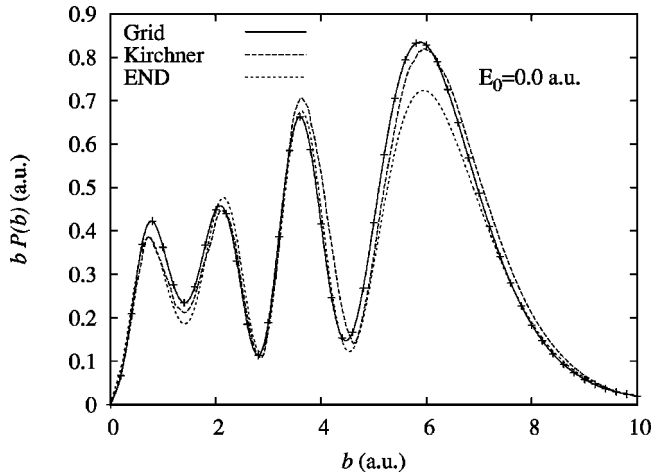

FIG. 3. $He^{2+}+H$ charge transfer probability as a function of the impact parameter b with no laser field for a projectile energy of 8 keV. Kirchner's data are taken from Ref. [6]. The symbols represent the calculated points in the impact parameter grid.

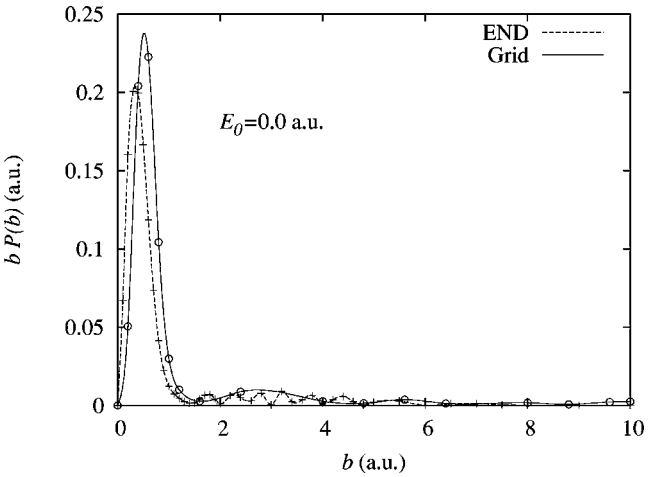

FIG. 4. Comparison of the grid and the END calculations: $He^{2+}+H$ weighted collision-induced charge transfer probability ($E_0=0$ a.u.) as a function of impact parameter b for a collision energy of 1 keV. The symbols represent the calculated points in the impact parameter grid.

III. RESULTS

The parameter space of laser-assisted charge transfer processes is formed by the scattering parameters of the collision, the impact parameter b and projectile velocity v, and the laser parameters, the frequency ω, peak intensity I_0, pulse duration τ, and polarization. In this work, we fix the projectile velocity at $v=0.1$ a.u. (1 keV). We also fix the frequency, $\omega=0.057$ a.u. (corresponding to $\lambda\approx 800$ nm) and the peak intensity at $I_0=3.5\times 10^{12}$ W/cm^2. The pulse is a Gaussian with a FWHM of 6 fs. This pulse length was chosen only for computational convenience, however, and we expect the results to held for longer pulses as well. The key point is that the collision time is on the order of a single optical cycle. Combined with the fact that the laser has essentially zero probability of exciting or ionizing either collision partner at this intensity, we conclude that the dependence of our results on the pulse length is weak so long as the pulse is more than a few optical cycles long. As a consequence, much longer pulses can be used—and still achieve the assumed intensity—easing experimental timing issues.

We have studied both collinearly and perpendicularly polarized (with respect to the projectile trajectory) laser fields. For the latter case, calculations were performed for different angles α between the laser field and the collision plane (Fig. 1). Since the collision time is roughly one or two optical cycles, even for the relatively slow projectile under consideration, the laser pulse effectively becomes a few cycle pulse. It follows that the phase of the laser field at the time of closest approach, the RCLP, can also influence the reaction. It is unlikely, however, that the RCLP can be either controlled or determined experimentally. The experimental observable is thus the RCLP averaged results, although we will also present the RCLP dependent results.

A. Testing

Before turning to the discussion of the results, we address the question of the validity of our calculations.

We first compare our results with those of Kirchner [6] for $He^{2+}+H$ charge exchange with no laser field and a projectile velocity of $v=0.283$ a.u. (8 keV). The results are shown in Fig. 3. Small deviations of our lattice calculations from Kirchner's calculations are evident but result in less than a 1% difference for the charge exchange cross section. Such agreement is within our target accuracy for this work.

We also compare our grid results with the END calculations in Fig. 3. Although the agreement with Kirchner's calculations is not as close as for the grid calculations, the difference in total cross section is still within 6%. This difference is likely due to the fact that the Gaussian basis set is not sufficiently diffuse to properly describe the tail of the wave function.

In Fig. 4, we show the weighted charge transfer probability induced by the collision ($E_0=0$ a.u.) as a function of the impact parameter b for a collision energy of 1 keV for both the grid and END methods. The END cross section for this case is $\sigma=0.80$ a.u.^{2} which agrees well with the grid method result of $\sigma=0.94$ a.u.^{2}. As Fig. 4 shows, the major discrepancy between the grid and END calculations comes from the region $b<2$ a.u., which is precisely where one might expect the straight line trajectory approximation to break down. Indeed, the END calculations show that for $b<2$ a.u. the trajectory can deviate from a straight line by as much as 14°. Even with these differences, the cross sections from the grid and the END methods are in reasonable agreement. Moreover, the main effect of the laser field will be to enhance the capture probability at large impact parameters where the straight line trajectory works well, leading to even better agreement between the cross sections. The discrepancy can also be partially attributed to the smaller number of impact parameters in the grid calculations, which leads to a less accurate evaluation of the cross section.

B. Parallel polarization

We have performed several calculations with the laser field polarized along the projectile trajectory. These are

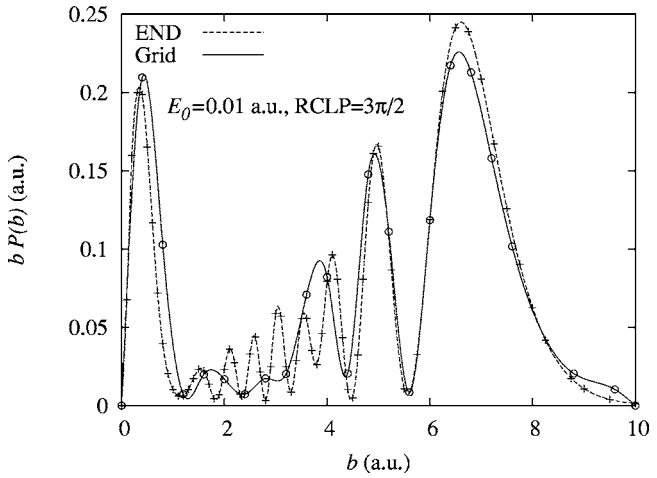

FIG. 5. Comparison of the grid and the END calculations: He^{2+}+H weighted laser-induced charge transfer probability as a function of impact parameter b for a collision energy of 1 keV, E_0=0.01 a.u., ω=0.057 a.u., and RCLP=$3\pi/2$.

shown in Fig. 5, where we note that both the END and the grid calculations suggest a dramatic enhancement in the reaction probability for large impact parameters when a moderately intense laser is added to the system (compare with Fig. 4). The END electron capture cross section is σ=4.5 a.u.^{2} which agrees well with the grid result of σ=4.7 a.u.^{2}. The difference can again be partially attributed to the smaller number of impact parameters in the grid calculations which miss some of the oscillations at intermediate b. Having gained confidence that our calculations correctly describe the effect of the laser on the charge exchange cross section, we turn to a more detailed study of the laser effects in He^{2+}+H charge exchange.

Since the laser peak intensity and wavelength are fixed, the only variable parameter is the RCLP. Even though it is unlikely that the experiment is possible, one interesting question is how the RCLP affects the reaction probability. In Fig. 6 we show the weighted capture probability as a function of

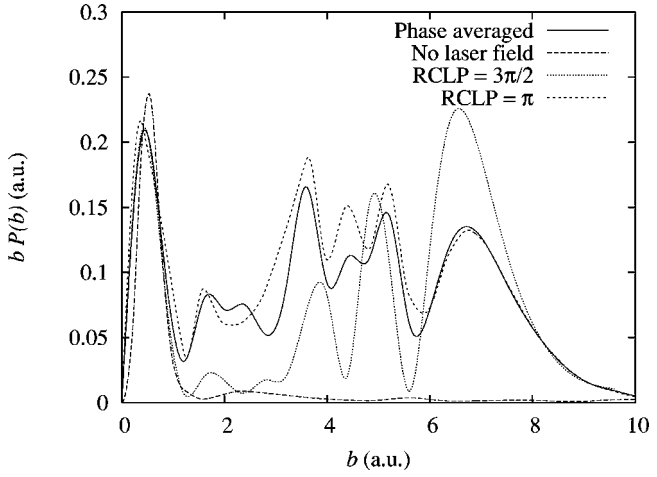

FIG. 6. Parallel polarization: He^{2+}+H weighted charge transfer probability as a function of impact parameter b for a collision energy of 1 keV (E_0=0.01 a.u. and ω=0.057 a.u.).

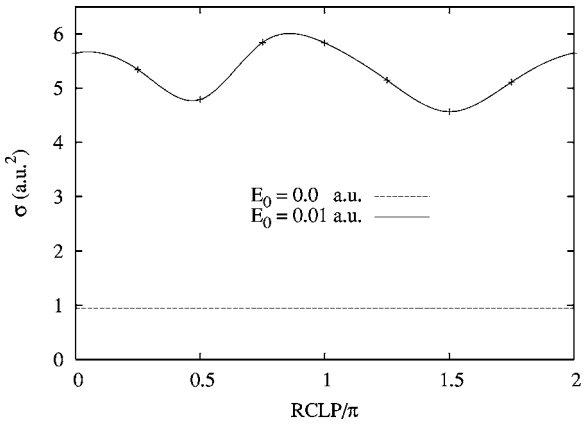

FIG. 7. Parallel polarization: He^{2+}+H charge transfer cross section as a function of the relative collision laser phase, φ (solid line) for a collision energy of 1 keV (E_0=0.01 a.u. and ω=0.057 a.u.). The dashed line is the free-field charge exchange cross section.

the impact parameter calculated for two values of the RCLP. For all impact parameters greater than 1 a.u., the laser field significantly enhances the capture probability, no matter what the RCLP is, in agreement with Kirchner's conclusions [6]. Although the capture probability varies significantly with the RCLP, all are larger than the field free result. This enhancement can be clearly seen in Fig. 7, where we show the capture cross section dependence on the RCLP. These results are in qualitative agreement with Kirchner's results [7], where he finds an enhancement of an order of magnitude at a higher frequency (ω=0.1 a.u.) and a higher intensity (E_0=0.02 a.u. or $I_0=1.4\times10^{13}$ W/cm^2) for the projectile energy of 1 keV. Averaging over the RCLP, which corresponds to the experimentally measurable quantity, we predict about a fivefold enhancement of the capture cross section (σ=5.28 a.u.^{2}) for a peak laser intensity of 3.5×10^{12} W/cm^2 and parallel polarization.

C. Perpendicular polarization

When the laser is polarized perpendicular to the projectile trajectory, one more parameter appears: the angle α between the laser polarization and the collision plane (See Fig. 1). The strong variation of the capture probability with α is evident from Fig. 8. This figure—and all results for perpendicular polarization—are based on the lattice solutions alone.

There, we show the RCLP-averaged capture probability as a function of the impact parameter for different relative polarization angles. Like the case of parallel polarization, the capture probability increases significantly for large impact parameters. This increase however, strongly depends on α. For polarizations close to the collision plane, we observe a large probability compared to the laser-free case, but the enhancement is much smaller when the polarization is nearly perpendicular to the collision plane. The full α dependence of the RCLP-averaged cross section can be seen in Fig. 9. Indeed, the maximum is about an eightfold increase for polarization in the collision plane (α=0 and $\alpha=\pi$), whereas the enhancement at $\alpha=\pi/2$ and $3\pi/2$ is no more than 10% based on the fitted curve. The α-averaged cross section is

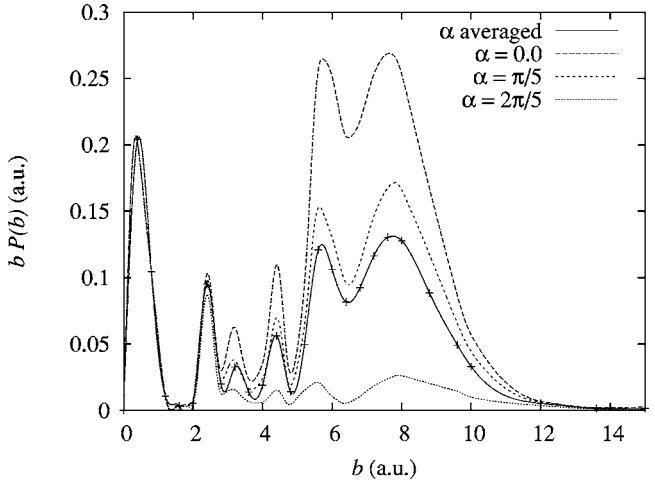

FIG. 8. Perpendicular polarization: RCLP-averaged, weighted charge transfer probability as a function of the impact parameter for different relative polarization angles α for a collision energy of 1 keV (E_0=0.01 a.u. and ω=0.057 a.u.).

four to five times larger than the laser-free case, and is thus comparable to the parallel polarization cross section.

An interesting feature of the relative polarization angle dependence is its symmetry. Although the symmetry due to reflection with respect to the collision plane ($\alpha \rightarrow 2\pi - \alpha$) is natural, the symmetry with respect to a plane perpendicular to the collision plane ($\alpha \rightarrow \pi - \alpha$) is not as obvious and deserves some discussion. In fact, this symmetry is the result of two simultaneous transformations that leave the Hamiltonian invariant: the geometrical transformation

$$\alpha \rightarrow \pi - \alpha$$

and transformation of the RCLP

$$\varphi \rightarrow \varphi + \pi.$$

The latter corresponds to inverting the direction of the laser field. It is the averaging over the RCLP that produces that extra symmetry of the phase-averaged cross section in Fig. 9.

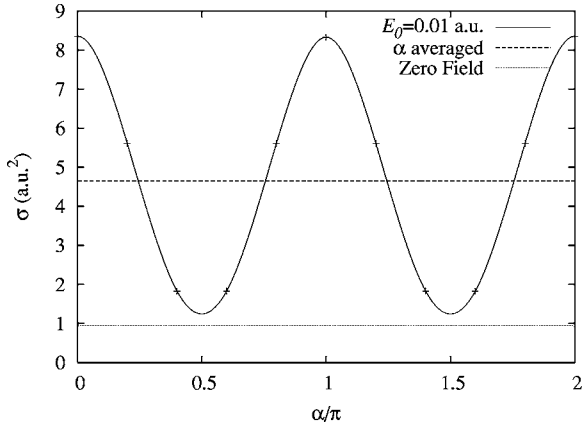

FIG. 9. Perpendicular polarization: phase-averaged cross section as a function of the angle α for a collision energy of 1 keV (E_0=0.01 a.u. and ω=0.057 a.u.).

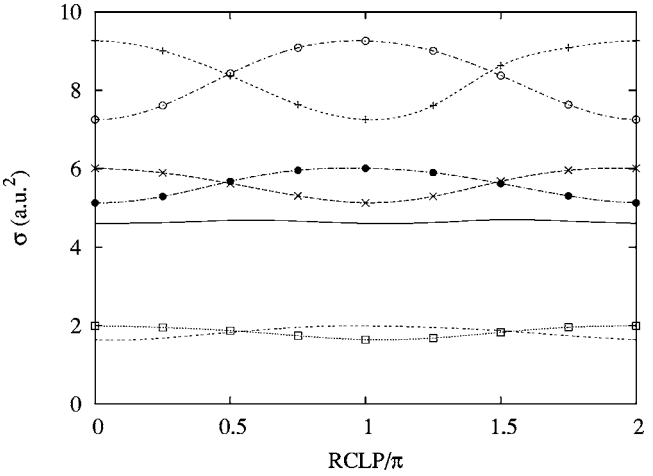

FIG. 10. Perpendicular polarization: capture cross section as a function of the laser phase for different α collision energy of 1 keV (E_0=0.01 a.u. and ω=0.057 a.u.). The α orientation angles are (+) α=0.0, (×) $\alpha=\pi/5$, (···) $\alpha=2\pi/5$, (□) $\alpha=3\pi/5$, (●) $\alpha=4\pi/5$, (○) $\alpha=\pi$, (—) α averaged.

Finally, let us address the question: How important is the RCLP in the case of perpendicular polarization? The answer to this question for the present parameters is given in Fig. 10. There we show the RCLP cross section dependence for different α. In agreement with Fig. 9, the strongest effect for all the orientations appears when the laser polarization lies in the collision plane. The RCLP effect in this case is also the strongest, but does not exceed 30% to 40%. The variation of the cross section with the RCLP decreases together with the enhancement when α is $\pi/2$ and $3\pi/2$, where both the RCLP variation and the enhancement are small. Averaging over α, we predict about a fivefold enhancement of the capture cross section (σ=4.66 a.u.^{2}) for a peak laser intensity of 3.5×10^{12} W/cm^2 and perpendicular polarization.

D. Simple physical picture

Given the large enhancements we have obtained, it is natural to wonder whether there is a simple physical explanation. We spent some effort to uncover such an explanation, and while we did not find a quantitative model, we did develop a qualitative model. This model plausibly explains many of the features seen in the numerical calculations, but is not yet a complete description.

In the limit that the laser field is slowly varying on the time scale of the collision, the collision can be modeled using the potential curves for the molecule in a static electric field. In the present case, the collision time at 1 keV (v=0.1 a.u.) is comparable to the laser period, 2.6 fs (110 a.u.), and the system experiences roughly two or three laser cycles during the collision. Thus, the present system is not strongly in the static field limit, and we believe this is the main reason that the model fails to describe some details of the numerical calculations. Correspondingly, we expect the model to work much better for faster collisions. In the opposite limit of a collision time very long compared to the laser period, the adiabatic Floquet potentials—which include the

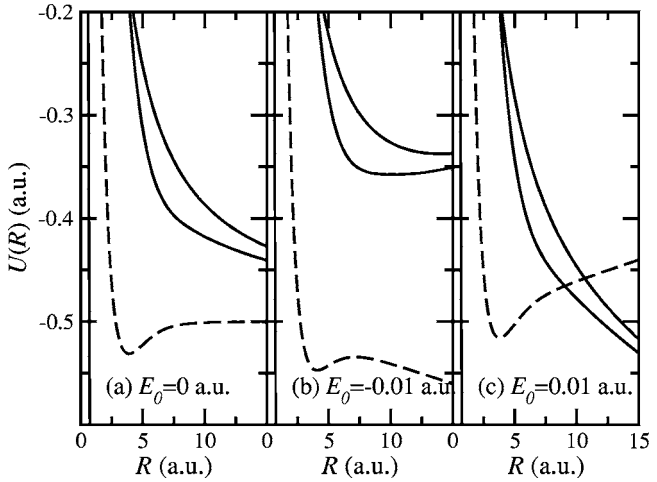

FIG. 11. The HeH^{2+} molecular potentials for (a) no electric field, (b) $E_0=-0.01$ a.u., and (c) $E_0=0.01$ a.u. The dashed line denotes the $He^{2+}+H(1s)$ initial state; the two higher-lying curves are the $He^{+}(2l)+H^{+}$ final states (solid lines). The HeH^{2+} ground state curve is also shown, but appears only as a vertical line near $R=1$ a.u.

effects of the oscillating electric field [17]—might provide a better starting point for a qualitative model.

The field-free potentials for the present case are shown in Fig. 11. The initial state $He^{2+}+H(1s)$ has a permanent dipole moment that is, to a good enough approximation for the present purpose, $-2R/5$; and the final states, $He^{+}(nl)+H^{+}$, $3R/5$. These moments can be most simply estimated from the charge distributions of the asymptotic channels, and refer to the nuclear center-of-mass frame. So, when the dipole interactions $-\mathbf{E}\cdot\mathbf{d}$ are added to the molecular potentials, the $He^{2+}+H(1s)$ and $He^{+}(2l)+H^{+}$ potentials cross when the electric field points from the He^{2+} to the H^{+} ($E>0$, Fig. 11). For $E<0$, the curves do not cross (Fig. 11). Charge exchange occurs at these crossings if the states are coupled. For laser-assisted collisions, the coupling is due to the transition dipole moment which, in this case, decays exponentially and is negligibly small by about $R=12$ a.u. So, only when the electric field is strong enough to generate crossings at $R<12$ a.u. will charge exchange be enhanced. Clearly, this enhancement comes at larger impact parameters, consistent with the numerical calculations. The $b\approx 12$ a.u. cutoff is also consistent with the numerical calculations.

Applying this model to the collision requires more care, however, because the electric field important for the σ-σ transitions of the above discussion is the projection along the internuclear axis (the component perpendicular to the internuclear axis is important for σ-π transitions). This projection changes during the collision since the internuclear axis rotates with respect to the lab-fixed laser polarization. For parallel polarization (see Fig. 1), the relevant electric field projection is thus

$$E_{\parallel}(t) = E_0 \frac{vt}{R} \tag{8}$$

while for perpendicular polarization it is

$$E_{\perp}(t) = E_0 \cos\alpha \frac{b}{R}. \tag{9}$$

The latter expression does explain the α dependence found numerically and shown in Fig. 10. It also suggests that the enhancement does indeed vanish at $\alpha=\pi/2$ and $3\pi/2$.

To the extent that the above features are generic to any heteronuclear collision system, we can expect enhancement in the charge exchange cross section. The primary question is how large a field is needed to push the field-induced crossings to small enough values of R that the transition dipole is non-negligible. The answer will depend on the field-free energy splitting of the initial and final states and the magnitude of their dipole moments.

It is worth emphasizing that since the time scale of the present collision lies between the static field and Floquet limits, our simple model should not be expected to explain all of the details of the numerical results. It does plausibly explain, though, why the capture cross section is enhanced at large impact parameters even at such relatively weak laser intensities. It also explains the α dependence for capture. The model's main shortcoming is that it does not predict the correct RCLP dependence for parallel polarization.

The failure of the model for the RCLP dependence is likely due to the fact that there are actually a few oscillations of the laser field during the collision. This time-dependence can be accounted for in our model by allowing the potentials in Fig. 11 to be defined by the instantaneous electric field, i.e., by allowing E_0 in Eqs. (8) and (9) to be time dependent. The resulting potentials then exhibit crossings, like those in Fig. 11(c), that move in time. Only when the nuclear trajectory $R(t)$ actually passes through this moving crossing—and at small enough R that the transition dipole moment is not negligible—will a transition occur. It turns out that for the present collision there are typically two or three such times. Moreover, the relative velocity between the moving crossing and the moving nuclei is different in each case as is the relevant transition dipole moment. The crossings thus vary between diabatic and adiabatic, making it difficult to develop quantitative estimates based on these ideas. Further complicating such estimates, the interferences between different paths through these crossings appear to be important.

Given the relatively small capture probabilities, it is also tempting to develop a quantitative estimate using perturbation theory. So, following Copeland and Tang [2], we used first order perturbation theory to approximately solve the time-dependent Schrödinger equation in the molecular basis including the laser field. The results, however, were in no better agreement with our numerical results than our simple model. The capture cross sections were enhanced with the laser field, but were overpredicted by a factor of 2 or more. Interestingly, the RCLP dependence predicted by perturbation theory is in rough agreement with the numerical results for parallel polarization, but not for perpendicular polarization—just opposite the case for our simple model. At the same time, though, the $P(b)$ from perturbation theory does not agree with the numerical results, even for parallel polarization.

The problem with this type of perturbation theory approach appears to be that the dipole matrix is included diabatically, but some of the crossings described above are more adiabatic. First order perturbation theory is insufficient for such crossings. On the other hand, diagonalizing the dipole matrix with the potentials to generate an adiabatic representation does not improve the first order approximation—the adiabatic crossings are better treated, but then the diabatic ones fail.

IV. SUMMARY

We have calculated the laser-assisted charge exchange cross section in the $He^{2+}+H$ collision based on a numerical solution of the three-dimensional Schrödinger equation on a grid. We show good agreement between our grid calculations, the END method, and the theoretical results of Kirchner [6]. The END method looks promising for calculations of laser-assisted charge exchange for systems with more than one electron and where trajectory effects are important.

We have studied two different laser polarizations for a moderate intensity (3.5×10^{12} W/cm^2) laser. Even for this relatively low peak intensity, we observe a strong, fourfold to fivefold enhancement of the charge transfer cross section with respect to a laser-free collision. In the case of parallel polarization the effect is slightly larger. Even though the collision time is roughly comparable to the period of the laser field, RCLP effects are not so important for observing the cross section enhancement.

Our calculations establish a substantial effect at "low" intensity, increasing our optimism that such an experiment can be done. To make the connection with experiment complete, however, we should perform an average over laser intensity to take into account the fact that the collision time relative to the laser pulse envelope cannot be controlled. Another average over laser intensity, to take into account the intensity variation across the laser focus, should also be performed. These tasks—which involve a substantial amount of computation—are the subject of future work.

ACKNOWLEDGMENTS

This work was supported by the Chemical Sciences, Geosciences, and Biosciences Division, Office of Basic Energy Sciences, Office of Science, U.S. Department of Energy. The authors are grateful to T. R. Coen for assistance in the early stages of this work and to K. D. Carnes, A. M. Sayler, and P. Q. Wang for critical comments and encouraging discussions. We especially appreciate detailed conversations with C. L. Cocke in the early stages and I. Ben-Itzhak more recently on the experimental aspects of this problem.

APPENDIX

As stated in the text, we initially used an explicit softening parameter in the Coulomb potentials to avoid the problems of singularity moving through the grid. The soft-core parameter a was included in the potential as follows

$$V=-\frac{Z_T}{\sqrt{x^2+y^2+z^2+a}}-\frac{Z_P}{\sqrt{(x-b)^2+y^2+(z-vt)^2+a}}. \tag{A1}$$

The soft-core parameter was varied from 0.0056 to 0.002 a.u.^{2} for two different impact parameters, $b=2.0$ a.u. and $b=6.0$ a.u., at 8 keV with no laser field. The original goal was to find the smallest value of a that give acceptably stable numerical results. The physical value, of course, is $a=0$. A few tests were enough to show that the capture probability was consistently overestimated for $a\neq0$. Plotting $P(b)$ as a function of a revealed that $P(b)$ was very close to a linear function of a. Figure 12 shows the results for both impact parameters. Extrapolating the linear fit to $a=0$ should thus give the physical result. For $b=2.0$ a.u., the extrapolation gave $P(2.0)=0.2261$. A calculation that had $a=0$ from the start yielded $P(2.0)=0.2240$. Similarly, for $b=6.0$ a.u., the calculated charge transfer probability $P(b)$ with no soft-core is $P(6.0)=0.1380$, and the result from the linear fit is $P(6.0)=0.1378$. So, the results found using two different approaches agree within 1% for both impact parameters.

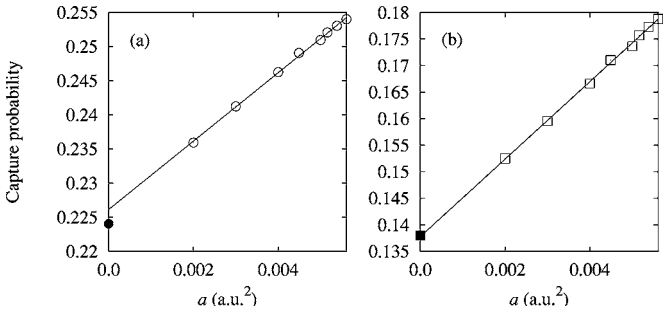

FIG. 12. Charge transfer probability as a function of the soft-core a for two different impact parameters: (a) $b=2.0$ a.u. and (b) $b=6.0$ a.u. for a projectile energy of 8 keV. The hollow symbols are the calculated points included in the fit (solid line). The filled symbol gives the calculated $a=0$ result.

Given the excellent agreement between the two approaches, we opted to use the less demanding, setting $a=0$ and choosing all b to lie midway between grid points (both impact parameters in the example above satisfied this criterion).

The linear behavior of the charge transfer probability as a function of the soft-core might make it possible to choose any value of b by using a soft-core. The charge transfer probability can then be calculated using a few values of a and extrapolating a linear fit to the $a=0$ limit. We did not, however, test this idea for arbitrary b. If it works, then the more accurate cross sections might be obtained by correctly reproducing all the oscillations in $P(b)$ (see Fig. 5).

[1] L. I. Gudzenko and S. I. Yakovenko, Sov. Phys. JETP **35**, 877 (1972).
[2] D. A. Copeland and C. L. Tang, J. Chem. Phys. **65**, 3161 (1976a).
[3] G. Ferrante, L. L. Cascio, and B. Spagnolo, J. Phys. B **14**, 3961 (1981).
[4] L. F. Errea, L. Méndez, and A. Riera, J. Chem. Phys. **79**, 4221 (1983).
[5] L. F. Errea, L. Méndez, and A. Riera, J. Chem. Phys. **85**, 825 (1986).
[6] T. Kirchner, Phys. Rev. Lett. **89**, 093203 (2002).
[7] T. Kirchner, Phys. Rev. A **69**, 063412 (2004).
[8] T. Kirchner, Nucl. Instrum. Methods Phys. Res. B **233**, 151 (2005).
[9] M. S. Pindzola, T. Minami, and D. R. Schultz, Phys. Rev. A **68**, 013404 (2003).
[10] T. Niederhausen, B. Feuerstein, and U. Thumm, Phys. Rev. A **70**, 023408 (2004).
[11] A. B. Voitkiv and J. Ullrich, J. Phys. B **34**, 1673 (2001).
[12] E. Deumens, A. Diz, R. Longo, and Y. Öhrn, Rev. Mod. Phys. **66**, 917 (1994).
[13] J. Broeckhove, M. D. Coutinho-Neto, E. Deumens, and Y. Öhrn, Phys. Rev. A **56**, 4996 (1997).
[14] W. H. Press, S. A. Teukolsky, W. T. Vetterling, and B. P. Flannery, *Numerical Recipes*, 2nd ed. (Cambridge University Press, New York, 1992).
[15] T. H. Dunning, J. Chem. Phys. **90**, 1007 (1989).
[16] S. C. Cheng and B. D. Esry, Phys. Rev. A **72**, 022704 (2005).
[17] S. I. Chu and D. A. Telnov, Phys. Rep. **390**, 1 (2004).